Atmospheric Research 183 (2017) 351–361

Contents lists available at ScienceDirect

Atmospheric Research

journal homepage: www.elsevier.com/locate/atmosres

A two-year study of carbonaceous aerosols in ambient $PM_{2.5}$ at a regional background site for western Yangtze River Delta, China

Dong Chen [a], Hongfei Cui [a], Yu Zhao [a,b,*], Lina Yin [a], Yan Lu [a], Qingeng Wang [a,b]

[a] State Key Laboratory of Pollution Control & Resource Reuse and School of the Environment, Nanjing University, 163 Xianlin Ave., Nanjing, Jiangsu 210023, China
[b] Jiangsu Collaborative Innovation Center of Atmospheric Environment and Equipment Technology (CICAEET), Nanjing University of Information Science & Technology, Jiangsu 210044, China

ARTICLE INFO

Article history:
Received 22 April 2016
Received in revised form 7 July 2016
Accepted 2 September 2016
Available online 4 September 2016

Keywords:
Carbonaceous aerosols
SOC
Biomass burning
Emission controls
YRD

ABSTRACT

To analyze the characteristics of regional background carbonaceous aerosols in western Yangtze River Delta (YRD), hourly organic carbon (OC) and elemental carbon (EC) in fine particular matter ($PM_{2.5}$) were measured with a semi-continuous carbon analyzer at a suburban site in upwind Nanjing from June 2013 to May 2015. Relatively low OC, EC and OC/EC were observed compared to other studies conducted in Nanjing. The reasons include the limited primary emissions around the observation site, the improved emission controls in recent years, and the use of denuder to reduce positive artifact in OC measurement. Resulting from the stable atmosphere conditions and emission variations, the highest concentrations of carbonaceous aerosols were found in both winters, with average OC and EC observed at 11.8 ± 10.0 and 5.9 ± 3.4 μg/m^3 for the first one, and 8.1 ± 5 and 4.5 ± 2.4 μg/m^3 for the second one, respectively. Compared to 2013, reduced OC and EC were found in summer and autumn 2014, demonstrating the benefits of emission control polices implemented for the Nanjing Youth Olympic, while elevated OC observed in spring 2015 was attributed probably to the increased biomass burning. For the hazy event in winter 2013, the back trajectories of air masses suggested that heavy pollution were from eastern Jiangsu, northern Anhui and Jiangsu, downtown Nanjing, and Shanghai. Secondary aerosol formation played an important role indicated by the larger mass fraction of OC and increased OC/EC in $PM_{2.5}$ during the heavy pollution period. In the harvest season, biomass burning was estimated to contribute 51% and 16% of OC and EC concentrations, respectively.

1. Introduction

As a main component of $PM_{2.5}$ (particles with aerodynamic diameters <2.5 μm), carbonaceous aerosols including organic carbon (OC), elemental carbon (EC) and carbonate (CC) (Birch and Cary, 1996; Chow et al., 2001) play vital roles in visibility, radiative forcing and human health (Wilson and Spengler, 1996). EC (sometimes referred to as black carbon, BC) originates mainly from incomplete combustion of biomass and fossil fuels, and is an important factor in climate studies for its optical characteristic of solar radiation absorption (Bond and Bergstrom, 2006). OC contains hundreds of individual organic compounds and it typically comprises 10–50% of ambient $PM_{2.5}$ mass (Seinfeld and Pandis, 1998). OC comes both directly from combustion sources (described as primary organic carbon, POC) and chemical reactions in which gaseous volatile organic compounds (VOCs) are converted to pollutants in the particle phase (described as secondary organic carbon, SOC). Attributed only to local source, CC is much smaller in the mass fraction (Chow et al., 2005).

Relatively high concentrations of OC and EC were found in China for decades (Novakov et al., 2005; Cui et al., 2015). Located in eastern China, Yangtze River Delta (YRD) is one of the country's regions with the most developed city cluster and the heaviest air pollution (Yao et al., 2002; Chan and Yao, 2008). A series of field measurements on ambient carbonaceous aerosols were conducted in YRD cities including Shanghai (Feng et al., 2009; Zhao et al., 2015a; Wang et al., 2015a), Hangzhou (Cao et al., 2009) and Nanjing (Zhuang et al., 2014; Li et al., 2015; Wang et al., 2015b). Most previous studies, however, were based on filter-sampling and off-line measurement without diurnal variations, and missed information of dynamic evolution processes of carbonaceous aerosols within one day (Hu et al., 2012). In addition, current measurements in YRD regions were conducted mainly in urban areas or downwind from cities, and the results could be largely influenced by local sources (Yang et al., 2005a, 2005b; Zhang et al., 2011; Li et al., 2015). The knowledge on regional background of carbonaceous aerosols for YRD, which is important for understanding the impacts of emissions

* Corresponding author at: State Key Laboratory of Pollution Control & Resource Reuse and School of the Environment, Nanjing University, 163 Xianlin Ave., Nanjing, Jiangsu 210023, China.
E-mail address: yuzhao@nju.edu.cn (Y. Zhao).

http://dx.doi.org/10.1016/j.atmosres.2016.09.004
0169-8095/

on regional air quality, is still lacking. Recently, series of measures on emission abatement and pollution control have been conducted in YRD cities (Zhao et al., 2015b), while their effects on ambient OC and EC have seldom been analyzed. In this case, long-term observation with high temporal resolution is necessary in the region to explore the characteristics and sources of ambient carbonaceous aerosols and to reflect the influence of emission controls on those aerosols, for the period with pollution control gradually implemented.

In this work, therefore, we conducted a more than two-year observation on hourly concentrations of ambient OC and EC in Nanjing, the capital city of Jiangsu province located in the western YRD (Fig. S1a in the supplement), to improve the understanding of the sources and formation of OC and EC in fine particles, and to indicate the effectiveness of local and regional PM controls in YRD. Nanjing is the second largest city in central east China following Shanghai, with a total area of 6587 km^2 and population of 8 million in 2012 (NJNBS, 2013). Coal is the dominant pollution source in Nanjing, and the heavy industries including coal-fired power, cement, steel and refinery plants accounted for 96% of the city's total coal consumption (Zhao et al., 2015b). Traffic is another important anthropogenic source due to the rapid growth in vehicle population since 2010 (Qiu, 2015), and the number reached 1.7 million in 2014 (NJNBS, 2015). It was the first time that real-time measurement based on thermal-optical method was applied at a site that can be representative for regional background of YRD (Ding et al., 2013). Inter-annual and seasonal of OC and EC were characterized at the site. The contributions of SOC formation to $PM_{2.5}$ were investigated with EC-tracer method. The influence of given anthropogenic sources on carbonaceous aerosols were further evaluated combining other air quality and meteorology information.

2. Methods

2.1. Site description

As shown in Fig. S1a, ambient OC and EC were measured at a suburban site in the Xianlin Campus of Nanjing University in northeast Nanjing, roughly 20 km away from downtown (118°57′10″E, 32°07′14″N, NJU site). The site is set at the roof of the School of the Environment building (about 30 m above the ground level), and is about 300 m away from the G25 highway. Shown in Fig. S2 in the supplement are the precipitation and temperature data collected from Jiangsu Provincial Meteorological Bureau (data source: http://www.jsmb.gov.cn), and Fig. S3 the monthly wind data measured at NJU site (note data were missed at the end of 2014 and the first half of 2015 due to instrument malfunction). Given the prevailing winds from southeast and northeast, the site is located upwind Nanjing with limited effects of the local emissions in the downtown. Besides the site is downwind of the most developed YRD region including the mega city Shanghai and the Suzhou–Wuxi–Changzhou city cluster (Fig. S1b-d), thus it is representative for the regional level of western YRD (Ding et al., 2013).

Due to the technical problems of the instruments at NJU site, other species in the atmosphere including ozone (O_3), carbon monoxide (CO), sulfur dioxide (SO_2), nitrogen dioxide (NO_2), $PM_{2.5}$ and PM_{10} were routinely measured and reported at a state-operated monitoring site (Xianlin site), 4.5 km west from the NJU site (Fig. S1a). To evaluate the observation discrepancies at two sites, available simultaneous measurements on $PM_{2.5}$ mass concentrations at the two sites were collected and compared for July-Oct 2014 and Dec 2014, as shown in the Fig. S4. The hourly $PM_{2.5}$ concentrations were satisfyingly consistent with each other, and high correlation coefficients were calculated for both periods. Given the relatively close distance between the two sites, therefore, we assume that there was no significant difference in the air quality between NJU and Xianlin site, and the data at Xianlin sites could then be applied as an approximation for NJU.

2.2. OC and EC measurement

The OC and EC measurement was conducted continuously for two years from June 2013 to May 2015, covering summer: June–August of 2013 and 2014; autumn: September–November of 2013 and 2014; winter: December to February of 2013, 2014 and 2015; spring: March–May of 2014 and 2015. We refer the period of June 2013–May 2014 and that of June 2014–May 2015 as the first and the second year, respectively.

Hourly ambient concentrations of OC and EC in $PM_{2.5}$ were sampled and measured by semi-continuous carbon analyzer (Model-4, Sunset Lab, USA). The analyzer applies the thermal-optical transmittance (TOT) method and uses a modified protocol of the National Institute of Occupational Safety and Healthy (NIOSH 5040) as its default protocol. The airborne particles are first inhaled into a $PM_{2.5}$ cyclone at a flow rate of 8.0 l/min, with the collection time set at 40 min for each cycle. $PM_{2.5}$ then passes through a carbon impregnated multichannel parallel-plate diffusion denuder which removes the gas-phase organic compounds that may transform to solid-phase organic carbon to increase the positive artifact (Turpin et al., 2000). OC and EC were collected on two quartz filters to save the losing gas-phase organic compounds that originate from solid-phase under the destruction of gas-solid equilibrium (Huebert and Charlson, 2000; Cheng et al., 2009; Cheng et al., 2010). $PM_{2.5}$ on the filters were then analyzed following the NIOSH protocol and TOT method for carbon factions, including four OC fractions in a helium atmosphere and six EC fractions in a 2% oxygen/98% helium atmosphere. The correction for the pyrolyzed carbon (PC) converted from OC to EC was performed by monitoring the transmittance of a pulsed He-Ne diode laser beam at 660 nm through the quartz fiber filter during the sample analysis. At last, all the carbon components (OC and EC) were converted to CO_2 and detected with a non dispersive infrared (NDIR) absorption CO_2 sensor. OC and EC were automatically quantified by dividing their peak areas by the internal calibration peak made by methane gas (5% CH_4 in He). The resultant OC was the sum of OC fractions and PC, and EC was defined as EC fractions minus PC. The details of quality control and assurance are described in the supplement. In addition to thermal EC, an optical measurement of EC was also provided by the Sunset analyzer. The optical EC is calculated using the light attenuation (ATN) through the quartz filter monitored throughout the sampling time. The optical OC is calculated by subtracting optical EC from TC. However, to our knowledge, the light attenuation is not only caused by EC but also by brown carbon (BrC), and the optical EC may overestimate the true value. Thus the thermal EC and OC were applied to this study.

The original hourly OC and EC concentrations were judged according to the data before and after the moment. Outliers of OC and EC were excluded when it was ten times higher than the nearest two time points. Moreover, the averaged OC positive artifact in this study (0.89 μgC/m^3) was at the similar level with that by Lin et al. (2009) (0.94 μgC/m^3). The detection limit for OC and EC of the instrument were 2.0 μgC/m^3 and 0.5 μgC/m^3 according to Lin et al. (2009), thus the measured OC and EC concentrations lower than the detection limit were screened out in this study. Totally ~14,834 h of OC and EC valid data were available after screening.

In order to investigate the influence of sampling and analytical methods on results, 16 off-line daily $PM_{2.5}$ samples were collected using a four-channel sampler (TH-16 A, Tianhong Company, Wuhan, China) during March 5–23 in 2015, and were analyzed using the same protocol as the on-line measurement. In addition, 36 off-line $PM_{2.5}$ samples were collected in summer (August 13–September 4, 2013), winter (December 26–29, 2013), and spring (April 18–May 1, 2014) using TH-16 A, and were analyzed using a DRI Model 2001 Thermal/Optical Carbon Analyzer. The analyzer applies thermal-optical reflectance (TOR) method under Interagency Monitoring of Protected Visual Environments (IMPROVE_A) protocol (Chow et al., 2001). The results are compared with those from on-line measurements.

3. Results and discussions

3.1. Concentrations of OC and EC

As shown in Fig. S5a in the supplement, good correlations are found between the off-line and on-line carbonaceous aerosol samples with the same TOT_NIOSH method. The correlation coefficients for OC, EC and total carbon (TC, the sum of OC and EC) are calculated at 0.93, 0.94 and 0.94, respectively. However, the off-line OC concentrations were 1.9 times of on-line ones, as the use of denuder in on-line measurements partly removed the gas-phase organic compounds that were absorbed on the quartz filter, and thereby reduced the positive artifact in OC measurement (Turpin et al., 2000). The result is consistent with a previous observation study in Beijing which found that OC concentrations measured without a denuder were 100% larger than those with one (Hu et al., 2008). Fig. S5b shows good correlations between the results of offline samples measured with TOR_IMPROVE and online ones with TOT_NIOSH, indicating the consistency between the two analytical methods. The statistics of OC, EC and TC with the two methods are summarized and compared in Fig. S5c (note the OC results of offline samples with TOR_IMPROVE are corrected by dividing the original values by 1.9, to remove the positive artifact). Similar TC levels are found for the two methods, while the EC from TOT_NIOSH was 24% lower than that from TOR_IMPROVE, because of the transmittance charring correction and a much higher peak inert mode temperature applied in the NIOSH protocol (Cheng et al., 2011).

Hourly OC and EC concentrations during the measurement period ranged from 1.01 to 83.67 and from 0.84 to 32.99 μg/m^3, respectively. Illustrated in Fig. S6 in the supplement, 83% of TC concentrations were in the range between 2.5 and 12.5 μg/m^3. As shown in Table 1, the OC and EC concentrations and the OC to EC ratios (OC/EC) measured in this work were slightly lower than most other available studies in Nanjing, attributed mainly to the following facts. First, as shown in Fig. S1b-d, relatively low emission intensities of primary $PM_{2.5}$, OC and BC were found around the NJU site, as it is located in the suburban area between downtown Nanjing and the developed Suzhou–Wuxi–Changzhou city cluster. Second, as described in Section 2.2, the use of denuder in this work partly reduced the positive artifact in OC measurement due to the absorption of gas-phase organic compounds, leading to lower OC/EC than previous measurements without denuder. Moreover, as the host city of Asian Youth Games 2013 and Youth Olympics Games 2014 (YOG), Nanjing have greatly implemented air pollution control policies for the most recent years (especially in 2014) including enhanced use of air pollutant control devices for big industrial sources and prohibition of biomass open burning, resulting in reduced emissions and thereby ambient concentrations of air pollutants. The effect of emission control for YOG on seasonal variation of carbonaceous aerosols is presented in Section 3.2.

Fig. 1 shows the mass fractions of hourly carbonaceous aerosols classified by $PM_{2.5}$ level during the studying periods. Based on a data sample size of >10,000, an approximate lognormal distribution is derived for frequency of $PM_{2.5}$ concentrations, and about half of them exceeded the national ambient air quality standard of 75 μg/m^3, reflecting heavy aerosol pollution in the area. Compared to smaller mass fractions (about 13%) for categories with high $PM_{2.5}$ levels (100–500 μg/m^3), larger mass fraction (about 41%) of carbonaceous aerosols in $PM_{2.5}$ is found for period relatively lower $PM_{2.5}$ levels (0–20 μg/m^3). The result indicates, on one hand, that rapid increase in other compounds like secondary inorganic aerosol (SIA) contributes significantly to heavy haze events, especially in the Yangtze River Delta area (Yang et al., 2011a, 2011b). On the other hand, the sharp increase in OC/EC along with enhanced $PM_{2.5}$ levels indicates a significant contribution of SOC which conversion from VOCs to haze events. Similarly, Zhang et al. (2016) found that the average OC/EC on hazy days (OC/EC = 4.2) was larger than that in non-haze days in Beijing (OC/EC = 3.4).

3.2. Seasonal variation of OC and EC concentrations

As shown in Fig. 2, compared to the second year, much higher concentrations of carbonaceous aerosols were observed in autumn and winter for the first year, at 11.0 ± 8.2 and 11.8 ± 10.0 μg/m^3 for OC, and 5.4 ± 3.0 and 5.9 ± 3.4 μg/m^3 for EC, respectively. In the second

Table 1
Summary of carbonaceous aerosol concentrations measured in ambient $PM_{2.5}$ (unless noted) in Nanjing.

Season	Sampling date	Site	Analytical method	OC (μg/m^3)	EC (μg/m^3)	OC/EC	Reference
Spring	Apr 2011	Urban	DRI-TOR	13.93	3.7	4.14	Wu et al. (2013)[a]
	Apr 2011	Suburban industrial	DRI-TOR	17.83	5.81	3.21	Wu et al. (2013)[a]
	Mar 2012	Urban	DRI-TOR	8.5	3.81	2.34	Li et al. (2015)
	Mar–May 2014	Suburban	Sunset-TOT	6.6	3.41	1.94	This study
	Mar–May 2015	Suburban	Sunset-TOT	7.99	2.83	2.82	This study
Summer	Jul 2011	Urban	DRI-TOR	11.41	2.17	5.74	Wu et al. (2013)[a]
	Jul 2011	Suburban industrial	DRI-TOR	9.53	1.77	5.86	Wu et al. (2013)[a]
	Jun 2012	Urban	DRI-TOR	7.57	3.09	2.53	Li et al. (2015)
	May–Jul 2013	Suburban	DRI-TOR	13	2.6	5.2	Duan et al. (2014)[a]
	Aug 2013	Suburban	DRI-TOR	10.06	2.27	5.25	Wang et al. (2014)[a]
	Jun–Aug 2013	Suburban	Sunset-TOT	6.52	4.09	1.59	This study
	Jun–Aug 2014	Suburban	Sunset-TOT	4.29	2.51	1.71	This study
Autumn	Sep 2001	Urban	Sunset-TOT	10.81	4.01	2.7	Yang et al. (2005a, 2005b)
	Oct 2011	Urban	DRI-TOR	12.08	2.42	5.06	Wu et al. (2013)[a]
	Oct 2011	Suburban industrial	DRI-TOR	13.24	2.69	5.09	Wu et al. (2013)[a]
	Nov 2011	Urban	DRI-TOR	18.1	6.6	2.8	Yuan et al. (2014)
	Nov 2011	Urban	DRI-TOR	15.72	5.9	2.76	Li et al. (2015)
	Sep–Nov 2013	Suburban	Sunset-TOT	10.98	5.4	2.03	This study
	Sep–Nov 2014	Suburban	Sunset-TOT	4.04	2.54	1.59	This study
Winter	Feb 2001	Urban	Sunset-TOT	15.63	3.3	4.73	Yang et al. (2005a, 2005b)
	Feb 2001	Suburban	Sunset-TOT	14.2	2.88	4.93	Yang et al. (2005a, 2005b)
	Jan 2011	Urban	DRI-TOR	13.75	4.43	3.16	Wu et al. (2013)[a]
	Jan 2011	Suburban industrial	DRI-TOR	13.17	4.67	2.77	Wu et al. (2013)[a]
	Dec 2013–Feb 2014	Urban	DRI-TOR	22.54	8.24	2.74	Li et al. (2015)
	Dec 2013–Feb 2014	Suburban	Sunset-TOT	11.62	6.01	1.93	This study
	Dec 2014–Feb2015	Suburban	Sunset-TOT	7.98	4.37	1.83	This study
Full year	Annual 2007–2008	Urban	DRI-TOR	15.7	10.4	2.36	Chen and Yin (2010)
	Annual 2010	Urban	DRI-TOR	–	–	1.92	Zhang et al. (2012)
	Annual 2014	Suburban	Sunset-TOT	5.69	3.2	1.78	This study

[a] The results indicate concentrations in $PM_{2.1}$.

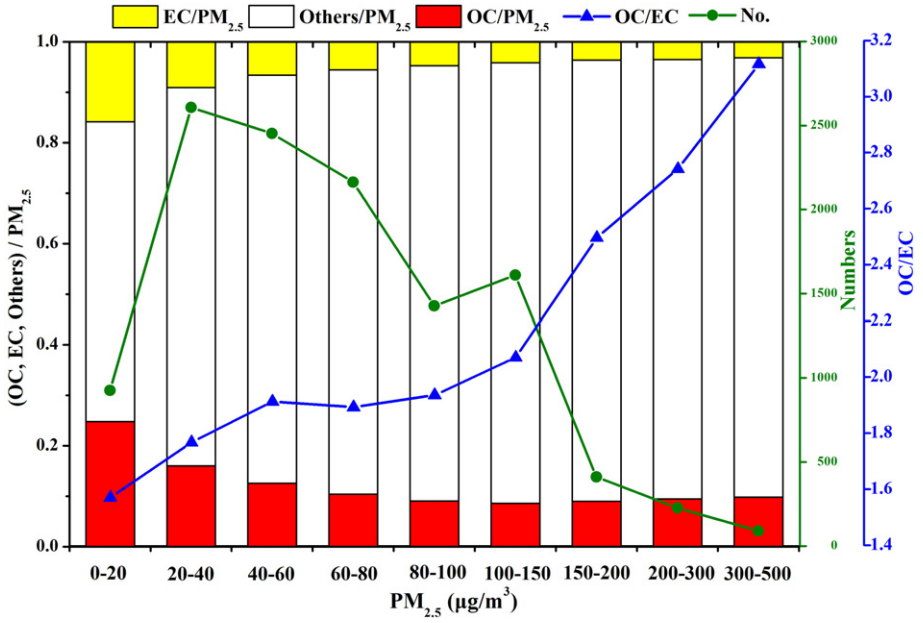

Fig. 1. The carbonaceous aerosol mass fractions of ambient $PM_{2.5}$ and OC/EC ratio, classified by $PM_{2.5}$ concentration at NJU site. Numbers of data points by $PM_{2.5}$ level are also shown.

year, winter and spring were the seasons with higher concentrations at 8.1 ± 5.0 and 8.3 ± 3.5 μg/m^3 for OC, and 4.5 ± 2.4 and 2.8 ± 1.3 μg/m^3 for EC, respectively. Similar to most cities across the country, both OC and EC levels were higher in winter and lower in summer, due to a combination of emissions and seasonal variance in meteorology (Cao et al., 2007). In summer, higher boundary layer in the atmosphere favors lower pollutant concentrations, and higher temperature results in a shift in the gas-particle equilibrium with more semi-volatile organic compounds (SVOCs) remaining in the gas phase (Yang et al., 2011a, 2011b). In addition, carbonaceous aerosols can also be effectively removed by wet deposition attributed to large amount of precipitation. In contrast, carbonaceous aerosol concentrations elevated in autumn and winter resulting from relatively stable atmospheric conditions, existence of temperature inversion, and variations in emissions. At −1 °C, for instance, the diesel vehicles were estimated to emit 7.6 times more OC than at 21 °C (Zielinska et al., 2012).

Remarkably, OC and EC concentrations declined from 6.5 and 4.1 in summer 2013 to 4.3 and 2.5 μg/m^3 in summer 2014, and from 11.0 and 5.4 in autumn 2013 to 4.0 and 2.5 μg/m^3 in autumn 2014. The concentrations then increased to 7.4 and 2.9 μg/m^3 for summer, and 7.5 and 3.4 μg/m^3 for autumn in 2015, respectively. The reduced concentrations in 2014 resulted from the control of anthropogenic emissions and the favorable meteorological conditions. In August 2014,series of more stringent measures than usual were conducted to improve air quality for YOG. Those measures included strict control on coal quality (all coal enterprises must use high quality coal with sulfur and ash content < 0.5% and 13%, respectively), entry prohibition of "yellow label" vehicles (the ones with extremely high emissions) into Nanjing, and expanded retirement or

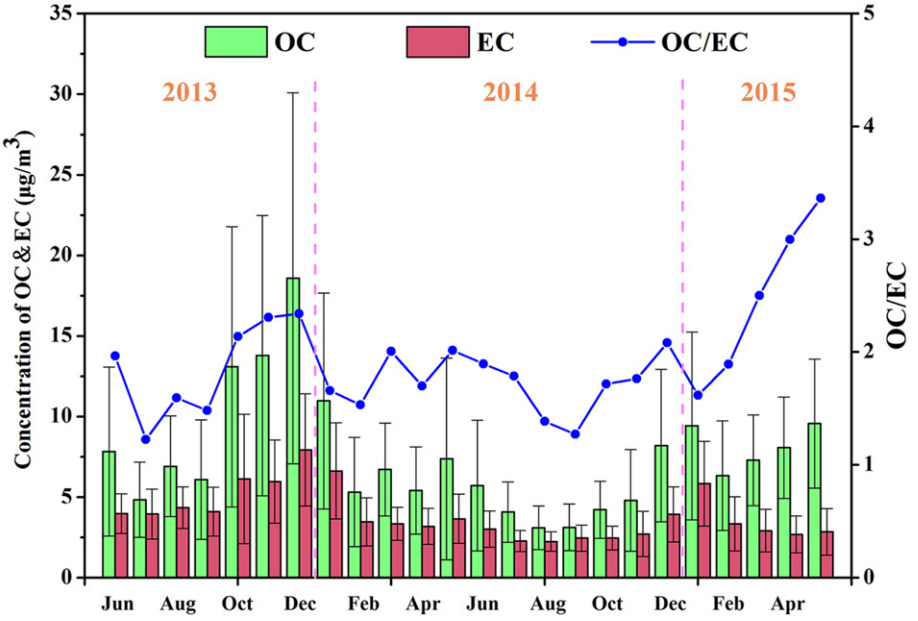

Fig. 2. Monthly variations of OC and EC concentrations and OC/EC ratios at NJU site in Nanjing from June 2013 to May 2015. Error bars denote the standard deviation of OC and EC concentrations.

Table 2
Correlation coefficients between concentrations of carbonaceous aerosol and other selected species from June 2013 to May 2015.

Period	Season		OC	EC	$PM_{2.5}$	PM_{10}	CO	NO_2	O_3	SO_2
Jun 2013–May 2014	Sum	OC	–	0.62	0.58	0.60	0.37	0.24	0.65	0.18
		EC	0.62	–	0.38	0.45	0.48	0.61	0.12	0.28
	Aut	OC	–	0.65	0.68	0.56	0.47	0.43	0.01	0.21
		EC	0.65	–	0.38	0.42	0.39	0.52	−0.18	0.13
	Win	OC	–	0.81	0.83	0.83	0.74	0.54	−0.23	0.38
		EC	0.81	–	0.74	0.78	0.31	0.67	−0.17	0.48
	Spr	OC	–	0.74	0.31	0.19	0.45	0.25	−0.03	0.17
		EC	0.74	–	0.27	0.23	0.54	0.54	−0.06	0.09
Jun 2014–May 2015	Sum	OC	–	0.70	0.63	0.62	0.50	0.45	0.48	0.37
		EC	0.70	–	0.49	0.51	0.43	0.65	0.04	0.51
	Aut	OC	–	0.74	0.80	0.74	0.55	0.53	−0.12	0.43
		EC	0.74	–	0.47	0.41	0.46	0.49	−0.25	0.10
	Win	OC	–	0.83	0.66	0.65	0.53	0.56	−0.20	0.46
		EC	0.83	–	0.61	0.62	0.36	0.67	−0.32	0.43
	Spr	OC	–	0.62	0.53	0.48	0.28	0.33	0.01	0.25
		EC	0.62	–	0.53	0.52	0.41	0.53	−0.22	0.29

limited production for industrial enterprise (e.g., 40% reduction of steel making for Nanjing Iron & Steel Group Corp). The emissions of primary $PM_{2.5}$, OC, EC and VOCs were estimated to decrease by 37%, 38%, 37% and 26% during YOG compared to the same period in 2013, and the concentrations of SO_2 and NO_2 decreased by 56% and 38%, respectively (Qiu, 2015). Not the SOC formation would be restrained attributed to the reduced VOCs emissions, and very low OC/EC was found in August 2014. Regarding meteorology, more precipitation in summer and autumn 2014 (752 mm) than 2013 (617 mm) (data source: http://www.jsmb.gov.cn) may elevate particle scavenging in the atmosphere and thereby lead to lower concentrations of carbonaceous aerosols.

Relatively high carbonaceous aerosol concentrations and OC/EC were observed in spring 2015. According to EARTHDATA (https://earthdata.nasa.gov/), much more fire counts were found in spring 2015 in Nanjing (1136) than those in winter 2014–2015 (114) or spring 2014 (852), indicating the increased contribution of biomass burning to ambient OC.

3.3. Correlation between carbonaceous aerosols and other pollutants

The correlation coefficients between concentrations of carbonaceous aerosols and other pollutants are calculated by season and shown in Table 2. Better correlation between EC and NO_2 was found than that between OC and NO_2 or between EC and SO_2 for all seasons except for autumn 2014. This result implies that traffic sources may play an important role in this region, since vehicles have relatively high emissions of both NO_X and EC (Hao et al., 2015). EC had stronger correlation with NO_2 than with CO (especially in winter). Given traffic NO_X and CO come mainly from diesel and gasoline vehicles, respectively (Yao et al., 2015), the result indicates that diesel vehicles, known as larger emitters of black carbon than gasoline ones (Casimiro et al., 2011), might be more influential in carbonaceous aerosol levels in this area. The correlation between OC and O_3 was strong in the summer 2014, implying that increased O_3 formation from high solar radiation may enhanced atmospheric oxidation and thereby the generation of SOC. In other seasons, however, negative correlations were found between carbonaceous aerosols and O_3, consistent with Latha and Badarinath (2004). The reason may be that the elevated concentrations of $PM_{2.5}$ and carbonaceous aerosols result in weakened solar radiation due to the extinction effects of aerosols, thus the O_3 formation is restrained.

Scatter plots of OC and EC and their correlation coefficients are shown by season in Fig. S7 in the supplement. For the first year, strong correlations between OC and EC was found for the winter (December 2013–February 2014; $R^2 = 0.66$) and spring (March 2014–May 2014; $R^2 = 0.55$), indicating that carbonaceous aerosols in the two seasons originated mainly from common sources and were influenced by similar

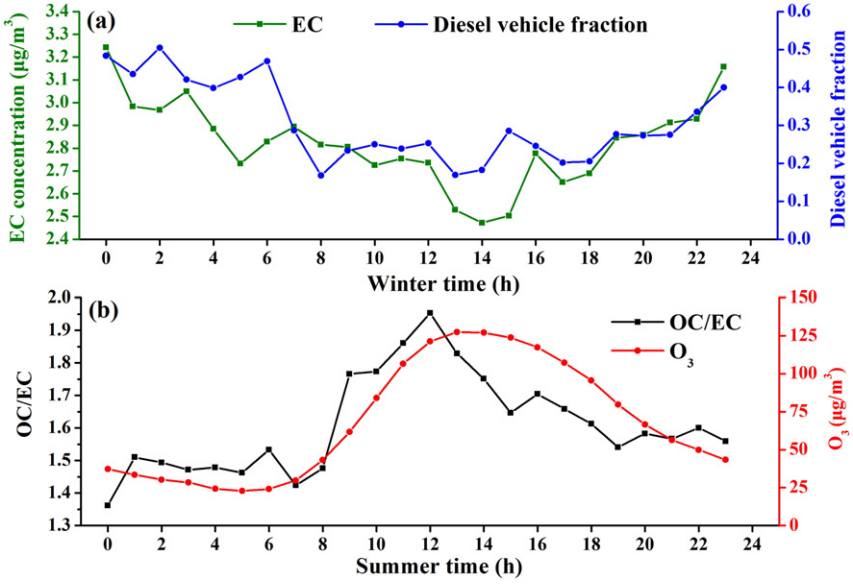

Fig. 3. The diurnal variation between carbonaceous aerosol and other reference materials during two typical seasons. (a) Diurnal variations of EC concentrations at NJU site and the fractions of diesel vehicles in G25 highway fleet in winter of 2015. (b) Diurnal variation of O_3 concentrations and SOC/OC in summer of 2013.

transport processes. The slopes of OC versus EC in winter (k = 2.09) and spring (k = 2.02) suggest the importance of coal combustion and vehicles in the area, as the primary OC/EC ratios were reported at 2.7 and 1.1 for the two types of sources, respectively (Watson et al., 2001). To test the impacts of motor vehicle on diurnal variation of carbonaceous aerosols, the fractions of diesel vehicles in the G25 highway were recorded with real-time camera in January 2015. As shown in Fig. 3a, strong association between hourly EC concentrations and diesel vehicle fractions was found ($R = 0.79$), particularly from 1700 to 2300 LT ($R = 0.97$), confirming the contribution of diesel vehicles on the ambient EC levels in winter. Relatively poor correlations in summer and autumn ($R^2 = 0.38$ and 0.44, respectively) imply more complicated and varied sources of OC and EC. In summer the accelerated SOC formation is a key factor leading to the poor correlation. As shown in Fig. 3b, the diurnal variations of O_3 and OC/EC in summer of 2013 were generally consistent with each other, and high OC/EC appeared at noon time (1100 to 1400 LT) in summers when solar radiation reaches peak, implying the contribution of increased atmospheric oxidation on SOC formation (Lin et al., 2009). For the second year, the correlation between OC and EC in winter remained strong ($R^2 = 0.69$) as shown in Fig. S7b, while better correlations were found in summer and autumn than those for the first year, implying reduced SOC generation. This partly ought to fewer emissions of gaseous precursors (i.e., VOCs) from the tightened controls for and after YOG.

To investigate the influences of pollution transport to Xianlin site, the relation between OC/EC ratios and wind directions from June 2013 to June 2014 is illustrated in Fig. 4a. Almost 70% of the OC/EC ratios were in the range of 0–2. The relatively low ratios suggest again the contribution of traffic sources on air quality in the area. Similar result was found in Hong Kong, where OC/EC ranged from 0.2–1.2 due to large emissions from diesel engines (Chow et al., 2005). The larger ratios (3–5 and >5) were associated mainly with northeastern winds. Compared to urban area with intensive traffic, the area northeastern to NJU site represents regional background level of air pollutants and the

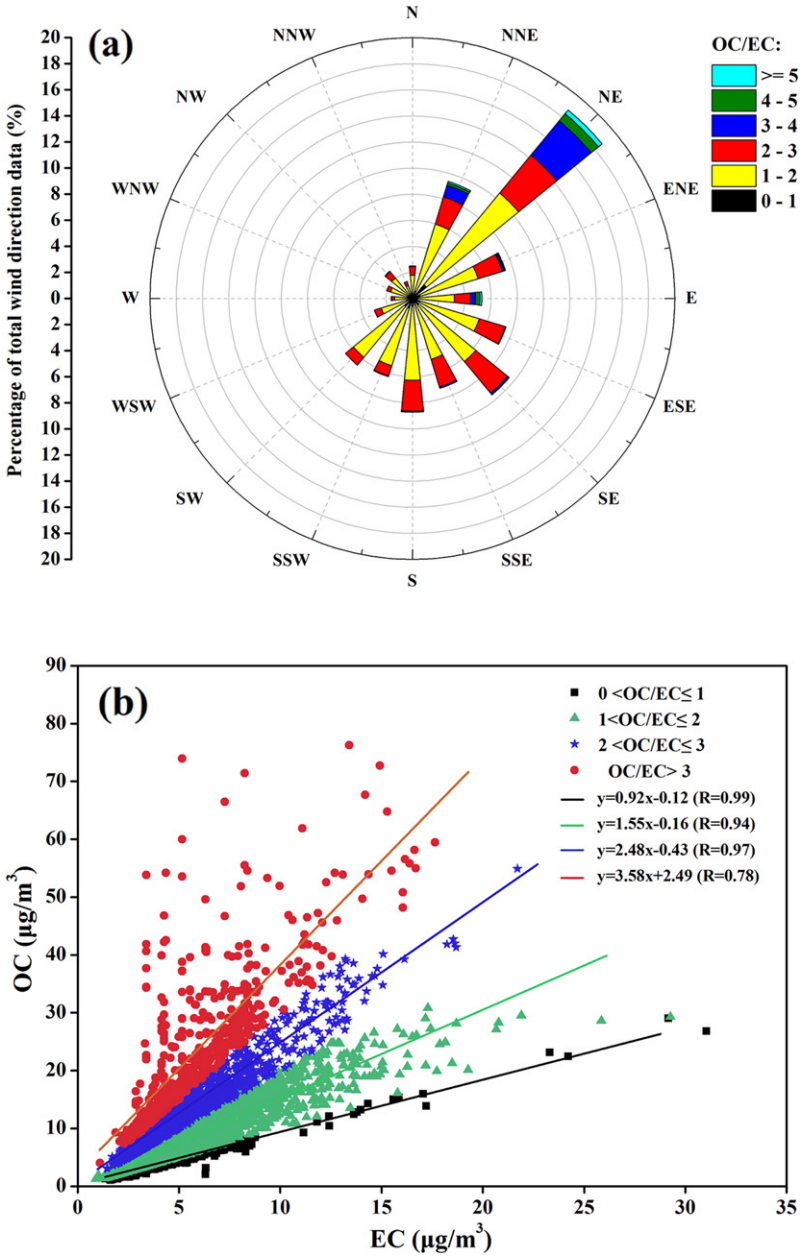

Fig. 4. (a) The observed OC to EC ratios associated with the wind directions at NJU site from June 2013 to June 2014. (b) Correlation between OC and EC concentrations classified by OC/EC interval.

precursors are more liable to be transformed to SOC, leading to the higher OC/EC (Cui et al., 2015). The correlations between OC and EC are re-analyzed by separating the OC/EC into four groups (≥3, 2–3, 1–2 and ≤1), as shown in Fig. 4b. The poorest correlation is found for the group with OC/EC ≥ 3, resulting mainly from elevated SOC formation as large amount of VOCs emissions were estimated in southwest Yangzhou and north Zhenjiang.

3.4. SOC estimation by the EC-tracer method

Lacking any direct analytical techniques to quantify ambient POC or SOC concentrations, several indirect methods have been used to estimate the latter, including semi-quantification with certain tracer, simulation with transport chemistry model, and source apportionment of primary OC (Strader et al., 1999). Directly emitted from incomplete combustion, EC is commonly taken as a tracer of primary OC and the EC-tracer method has been widely used (Turpin and Huntzicker, 1991; Lim and Turpin, 2002; Cabada et al., 2004). The method has limitations: it cannot obtain single OC/EC that represented a mixture of primary sources varying in time and space (Yuan et al., 2006). For instance, SOC will be overestimated when occurred biomass burning with high emission ratio of OC to EC (Ding et al., 2012). Despite of the limitation, EC-tracer method is believed to provide reasonable SOC level at monthly or seasonal average when high frequency measurements are conducted (Folidori et al., 2006). Based on the hourly data from on-line measurement, therefore, we apply the method to estimate SOC concentrations using Eq. (1):

$$SOC = OC - EC \times (OC/EC)_{primary} - N \quad (1)$$

where *OC* and *EC* are the measured ambient OC and EC concentrations, respectively; $(OC/EC)_{primary}$ is the ratio of primary OC and EC emissions with the contribution of SOC excluded (Castro et al., 1999), N is usually considered as the contribution of POC from non-combustion sources (meat cooking operations, biogenic sources, etc.) or sampling artifacts (Lin et al., 2009; Cabada et al., 2004).

Traditionally, $(OC/EC)_{primary}$ can be determined by various ways including the OC to EC ratio from emission inventory, OC to EC concentration ratio from observation when SOC formation is weak and thus the concentrations are dominated by emissions, or the lowest OC to EC concentration ratio during the observation (Castro et al., 1999). Revisions have been made to improve the $(OC/EC)_{primary}$ determination in China (Chen et al., 2014; Day et al., 2015; Hu et al., 2012). For example, Hu et al. (2012) estimated the correlation coefficients between SOC and EC to determine the $(OC/EC)_{primary}$ based on relatively large dataset from online measurement. In this work, the correlation coefficient between OC and EC at 0.95 was taken as a threshold, i.e., the observed hourly OC and EC concentrations with correlation coefficient larger than 0.95 are selected to calculate the $(OC/EC)_{primary}$. The calculated OC/EC ratios from the selected datasets were in the lowest 20% values from the whole datasets by season and year, in accordance with the suggestion of $(OC/EC)_{primary}$ determination by Cao et al. (2007). As shown in Fig. S8 in the supplement, the $(OC/EC)_{primary}$ were estimated at 1.03, 1.25, 1.53, and 1.07 for summer, autumn, winter and spring for the first year (June 2013–May 2014), and at 0.86, 1.06, 1.38, and 1.88 for summer, autumn, winter and spring for the second (June 2014–May 2015). To test the rationality of $(OC/EC)_{primary}$ determination, we followed the method by Cabada et al. (2004) and compared the NO_2 and CO concentrations for the "primary emission dominating" period (i.e., the period we chose for $(OC/EC)_{primary}$ estimation) and other period. As shown in Fig. S9, the concentrations in the primary emission dominating period were much larger than those in other period, implying that our estimation was reasonable. The annual averages of $(OC/EC)_{primary}$ are then calculated at 1.22 and 1.30 for the two years, respectively, slightly lower than the results from emission inventory at 1.38 for 2012 (Zhao et al., 2015b). Although Chow et al. (1996) suggested the OC/EC at 2.0 as a threshold to identify SOC formation, lower values have been applied in some studies in China. For example, Xiao et al. (2011) and Cao et al. (2004) used the value 1.1 as $(OC/EC)_{primary}$ in Pearl River Delta to separate POC and SOC, close to our estimates in western YRD region. Non-combustion POC could be determined by the intercept of the linear regression between OC and EC. According to Fig. 4 (b), the intercept of the regression line was only 0.4 μgC/m^3 on average from June 2013 to June 2014, and the ratio of N to OC was calculated at 4.6%. As SOC could also contribute to the intercept, non-combustion POC was thus believed to be smaller than 0.4 μgC/m^3 on average. Therefore we think the contribution of non-combustion sources to POC was not significant in this area.

The estimated SOC levels are illustrated by season in Fig. 5. Similar to downwind Nanjing (Li et al., 2015), the SOC concentrations at the upwind NJU site in the first year were higher in autumn and winter at 4.5 and 3.0 μg/m^3, respectively, resulting from the stable meteorological conditions that favor the accumulation of VOCs precursors. The fractions of SOC to OC (SOC/OC) were calculated at 0.45, 0.41, 0.34 and 0.26 for summer, autumn, spring and winter, respectively. Despite of lower concentrations, the larger SOC/OC ratio in summer indicated the enhanced SOC formation rate upon high temperature as mentioned before. Decreased SOC concentrations were found in summer, autumn and winter

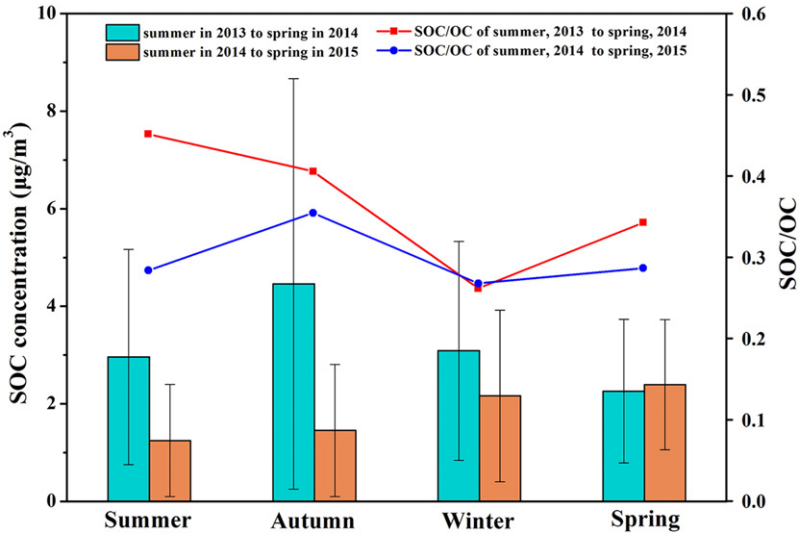

Fig. 5. Seasonal SOC concentrations and SOC/OC ratios from June 2013 to May 2015. Error bars denote the standard deviation of SOC concentrations.

of the second year resulting probably from the reduced precursor emissions and the stronger particle removal by increased precipitation.

3.5. The characteristics of carbonaceous aerosols during heavy haze and biomass burning periods

During the sampling period, the episodes of haze pollution were captured in the upwind Nanjing sites (Xianlin and NJU). Extremely serious air pollution occurred in YRD region in early December 2013 (Tang et al., 2016; Xu et al., 2015; Zhang et al., 2015). As shown in Fig. 6, the mean value of wind speed was <0.5 m/s during 2–9 December, and the hourly average concentrations of $PM_{2.5}$ kept at high levels around 252 μg/m^3, with the peak reaching 474 μg/m^3 on 6 December. High concentrations of NO_2 and SO_2 during 2–9 December implied the elevated secondary inorganic aerosol level for the serious pollution episode. Meanwhile, the fraction of OC in $PM_{2.5}$ for the same period was estimated at 12%, much higher than that of EC at 4%. Compared to the low OC/EC ratio in the cleaning days (1.5 for 10–11 December), the larger OC/EC ratio (3.2 for 2–9 December) indicated the notable contribution of SOC to $PM_{2.5}$ for the haze episode. As shown in Fig. S10 in the supplement, there were 7 types of air masses arriving at NJU site through the back trajectory analysis using the Hybrid Single Particle Lagrangian Integrated Trajectory (Hysplit, version 4.9) (http://www.arl.noaa.gov/ready.html). The 48-h air mass back trajectories were calculated using HYSPLIT for every hour from 4 December to 9 December starting at the observation site, and 48-h backward air mass trajectories at 30 m above the ground (the same as NJU site) were selected for cluster analysis. The OC, EC and $PM_{2.5}$ concentrations with trajectories numbers for each cluster are summarized in Table 3. Originated from eastern Jiangsu, downtown Nanjing, northern of Anhui and Jiangsu, and Shanghai, respectively, Clusters 1, 2, 3 and 5 collectively accounted for 77% of all the trajectories and were thus identified as the main air masses. All these four clusters of air masses moved slow and elevated contribution of regional sources to the $PM_{2.5}$ and carbonaceous aerosols levels. Air masses with faster moving velocities came from north China and coastal areas, e.g., Cluster 7 from the Siberia Plateau and Cluster 4 from eastern coastal areas. Accompanied with cold air and fewer pollutants, the OC, EC and $PM_{2.5}$ concentrations got low when the masses arrived at Nanjing. In general, the heavy pollution resulted from the poor meteorological conditions that prevented effective diffusion of local atmospheric pollutants, and the regional transport of air pollutants from the areas with intensive emissions.

Table 3
Numbers of backward trajectories and mass concentrations of carbonaceous aerosols and $PM_{2.5}$ in different air mass arriving at NJU site for 4–9 December, 2013.

Cluster	Number of trajectories	OC (μg/m^3)	EC (μg/m^3)	$PM_{2.5}$ (μg/m^3)
1	41	36	12	313.5
2	24	35.9	12.3	297.9
3	19	37.2	10.9	334.2
4	11	20.6	6.2	205.9
5	28	32.9	8	301.5
6	8	24.1	6.7	235.9
7	13	9	4	113

Biomass open burning after harvesting has significant impacts on regional air quality (Crounse et al., 2009), and carbonaceous aerosols are the key pollutants from the process (Jung et al., 2014). In most agricultural provinces in China, the biomass burning season is usually in June (Ni et al., 2015). Here we analyze the temporal trends of air pollutants from 20 May to 14 June 2014, to explore the impacts of biomass burning on air quality. Combining the observed pollutant concentrations, meteorological condition at NJU site, and fire counts in YRD region from Moderate Resolution Imaging Spectroradiometer (MODIS, https://earthdata.nasa.gov/data/near-real-time-data/firms), we divide the period to five sections (normal days I, biomass burning days I, cleaning days, biomass burning days II, and normal days II), as shown in Fig. 7. Note the biomass burning days are not determined based only on fire counts. For example, although there were only a few fire counts found in Anhui province near the NJU site on 30 May, the 24-h backward trajectory shows the air mass was exactly from the area (Fig. S11a in the supplement), and the elevated OC and EC were believed to be closely related to the open biomass burning. In contrast, there were much more fire counts in northern Anhui on 10 June, while OC and EC were not significantly elevated. The backward trajectory shows air mass on that day came from the eastern coastal areas where no fire count was found (Fig. S11b).

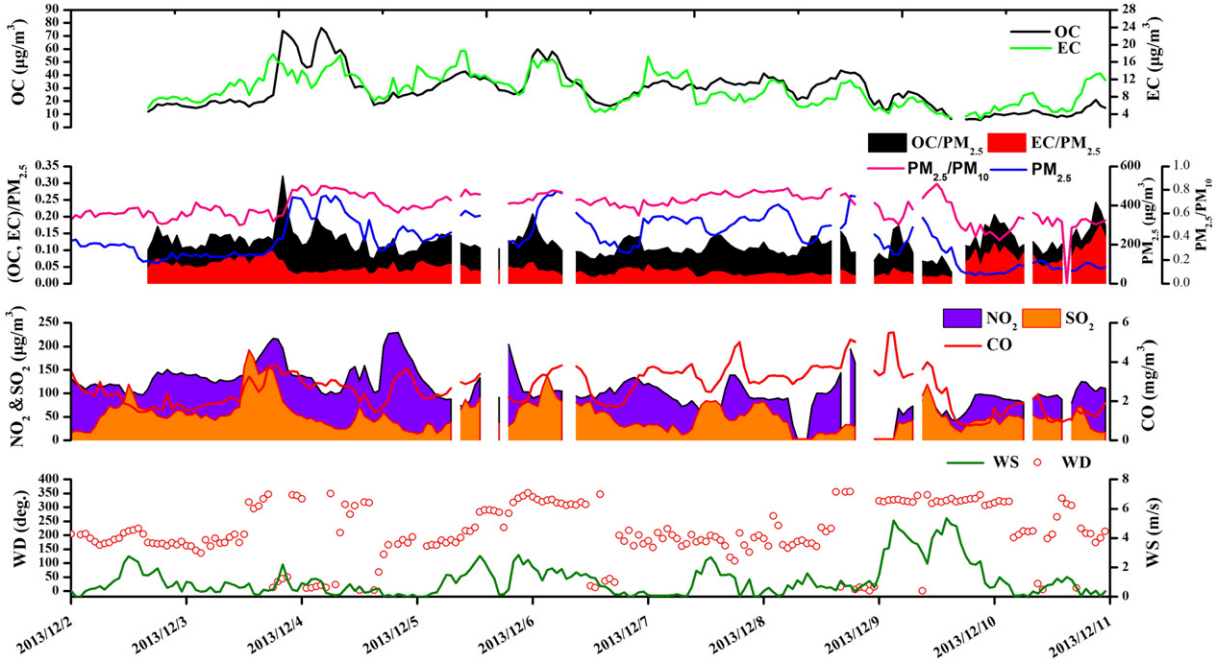

Fig. 6. The time series of hourly $PM_{2.5}$, OC, EC, CO, NO_2, SO_2 mass concentrations, the fraction of OC and EC in $PM_{2.5}$, and the wind direction and speed at upwind Nanjing sites for a heavy PM pollution episode in December 2013.

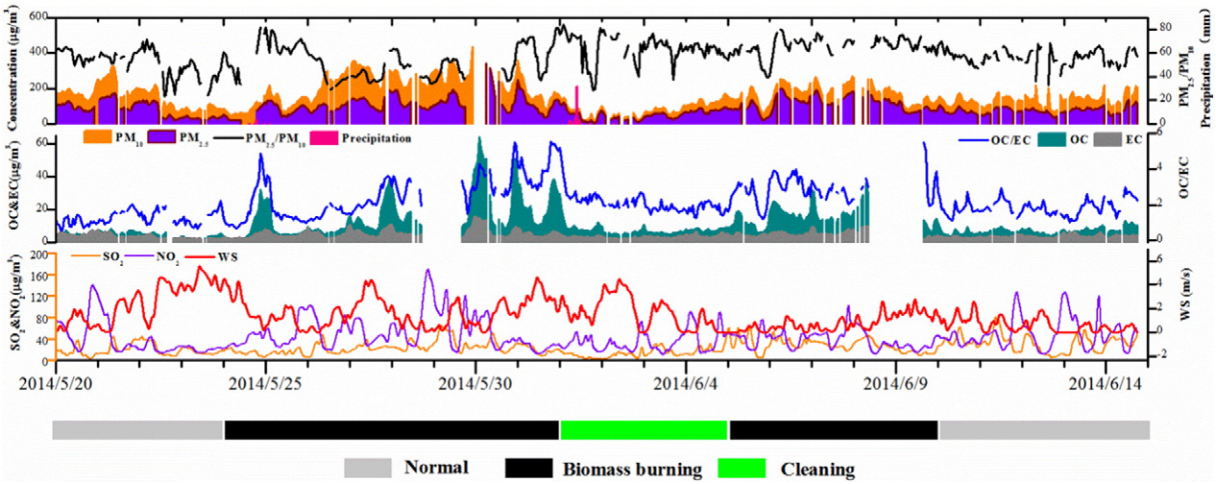

Fig. 7. The time series of hourly $PM_{2.5}$, PM_{10}, OC, EC, NO_2 and SO_2 mass concentrations, the $PM_{2.5}$ fraction in PM_{10}, OC/EC ratio and the meteorology conditions (wind speed and precipitation) at upwind Nanjing sites for a biomass burning period (20 May 2014–15 June 2014). The period was divided into three typical types: normal days (grey bar), biomass burning days (black bar), and cleaning days (green bar).

Summarized in Table 4 are the average concentrations of $PM_{2.5}$, OC, EC, and gaseous pollutants, as well as the ratios of OC to EC and the mass fractions of $PM_{2.5}$ to PM_{10} for the five sections. The concentrations of all the pollutants (except OC) were the lowest for cleaning days, attributed to the precipitation episode and high wind speed. For the biomass burning days, OC and EC concentrations increased by 157% and 41% compared to normal days, and $PM_{2.5}$ and PM_{10} exceeded the national ambient air quality standard (GB3095-2012) by 49% and 24%, respectively. In particular, the observed OC/EC ratios were much higher in biomass burning days, indicating the impacts of biomass burning on regional air quality and carbonaceous aerosols. We further quantify its contribution on OC and EC with Eq. (2), assuming the SOC formation rate is unchanged in normal and biomass burning days:

$$(OC/EC)_{obs} = (OC/EC)_{nbb} \times (1-\eta) + (OC/EC)_{bb} \times \eta \quad (2)$$

where $(OC/EC)_{obs}$ and $(OC/EC)_{nbb}$ are the observed OC/EC ratios during biomass burning and normal days, respectively; $(OC/EC)_{bb}$ is the ratio of OC to EC emission factors of biomass burning; and η represents biomass burning contribution rate of EC total emissions. Setting $(OC/EC)_{bb}$ at 8.32 (Li et al., 2007), the contribution rates of biomass burning to OC and EC in biomass burning days were calculated at 51% and 16%, respectively.

4. Conclusions

Carbonaceous aerosols in ambient $PM_{2.5}$ were continuously measured for two years at a regional background site in the western YRD region. Relatively low and decreased OC and EC were observed, attributed mainly to the improved emission controls in the area for recent years. Higher concentrations found in winter resulted from the stagnant atmosphere and emission variations. OC and EC were found to be well correlated in winters, indicating the common sources of coal combustion and traffic, while elevated SOC formation rate might weaken the correlation in summers. Based on the EC-tracer method, the largest SOC fraction to OC were estimated for summer, although the absolute SOC levels were the highest in autumn and spring for June 2013–May 2014 and June 2014–May 2015, respectively. Indicated by the mass fraction of OC in $PM_{2.5}$ and the sharp increase in OC/EC, formation and accumulation of secondary aerosols was identified as an important source of extremely hazy events in winter. In harvest season in summer, however, the increased carbonaceous aerosols came largely from the primary emissions of biomass burning, which was estimated to account for half of ambient OC in the period.

Acknowledgement

This work was sponsored by the Natural Science Foundation of China (41575142), Natural Science Foundation of Jiangsu (BK20140020), Jiangsu Science and Technology Support Program (SBE2014070918), and Special Research Program of Environmental Protection for Commonweal (201509004). Thanks should also go to two anonymous referees for their very valuable comments and suggestion to improve this work.

Appendix A. Supplementary data

Supplementary data to this article can be found online at http://dx.doi.org/10.1016/j.atmosres.2016.09.004.

Table 4
Statistics of particulate matter, carbonaceous aerosol, and gaseous pollutant concentrations, and OC to EC ratios during the biomass burning period (20 May–14 June 2014). See Fig. 7 for the dates of normal, biomass burning, and cleaning days.

		$PM_{2.5}$ ($\mu g/m^3$)	PM_{10} ($\mu g/m^3$)	$PM_{2.5}/PM_{10}$	SO_2 ($\mu g/m^3$)	NO_2 ($\mu g/m^3$)	OC ($\mu g/m^3$)	EC ($\mu g/m^3$)	OC/EC
Normal days	I	83.42	154.87	51.76	19	41	4	3.31	1.27
	II	78.87	142.08	56.11	31	50	6.05	3.29	1.86
	Average	81.14	148.47	53.93	25	45	5.02	3.3	1.57
Biomass burning days	I	108.11	201.02	52.16	22	52	12.82	4.72	2.49
	II	115.28	171.78	65.91	29	38	13.03	4.59	2.85
	Average	111.69	186.4	59.03	26	45	12.92	4.65	2.67
Cleaning days		52.88	80.77	64.07	19	34	6.22	2.98	2.12

References

Birch, M.E., Cary, R.A., 1996. Elemental carbon-based method for monitoring occupational exposures to particulate diesel exhaust. Aerosol Sci. Technol. 25, 221–241.

Bond, T.C., Bergstrom, R.W., 2006. Light absorption by carbonaceous particles: an investigative review. Aerosol Sci. Technol. 40, 27–67.

Cabada, J.C., Pandis, S.N., Subramanian, R., Robinson, A.L., Polidori, A., Turpin, B., 2004. Estimating the secondary organic aerosol contribution to $PM_{2.5}$ using the EC tracer method. Aerosol Sci. Technol. 38, 140–155.

Cao, J.J., Lee, S.C., Ho, K.F., Zou, S.C., Fung, K., Li, Y., et al., 2004. Spatial and seasonal variations of atmospheric organic carbon and elemental carbon in Pearl River Delta Region. China Atmos. Environ. 38, 4447–4456.

Cao, J.J., Lee, S.C., Chow, J.C., Watson, J.G., Ho, K.F., Zhang, R.J., et al., 2007. Spatial and seasonal distributions of carbonaceous aerosols over China. J. Geophys. Res. 112, 2156–2202.

Cao, J.J., Shen, Z., Chow, J.C., Qi, G., Watson, J.G., 2009. Seasonal variations and sources of mass and chemical composition for PM_{10} aerosol in Hangzhou, China. Particuology 7, 161–168.

Casimiro, P., Mário, C., Roy, M.H., Teresa, N., Fátima, M., Célia, A., et al., 2011. OC/EC ratio observations in Europe: Re-thinking the approach for apportionment between primary and secondary organic carbon. Atmos. Environ. 45, 6121–6132.

Castro, L.M., Pio, C.A., Harrison, R.M., Smith, D.J.T., 1999. Carbonaceous aerosol in urban and rural European atmospheres: estimation of secondary organic carbon concentrations. Atmos. Environ. 33, 2771–2781.

Chan, C.K., Yao, X.H., 2008. Air pollution in mega cities in China. Atmos. Environ. 42, 1–42.

Chen, K., Yin, Y., Wei, Y.X., Yang, W.F., 2010. Characteristics of carbonaceous aerosols in $PM_{2.5}$ in Nanjing. China Environ. Sci. 20, 1015–1020 in Chinese.

Chen, Y., Xie, S.D., Luo, B., Zhai, C.Z., 2014. Characteristics and origins of carbonaceous aerosol in the Sichuan Basin. China Atmos. Environ. 94, 215–223.

Cheng, Y., He, K.B., Duan, F.K., Zheng, M., Ma, Y.L., Tan, J.H., 2009. Positive sampling artifact of carbonaceous aerosols and its influence on the thermal-optical split of OC/EC. Atmos. Chem. Phys. 9, 7243–7256.

Cheng, Y., He, K.B., Duan, F.K., Zheng, M., Ma, Y.L., Tan, J.H., et al., 2010. Improved measurement of carbonaceous aerosol: evaluation of the sampling artifacts and inter-comparison of the thermal-optical analysis methods. Atmos. Chem. Phys. 10, 8533–8548.

Cheng, Y., He, K.B., Duan, F.K., Zheng, M., Du, Z.Y., Ma, Y.L., et al., 2011. Ambient organic carbon to elemental carbon ratios: influences of the measurement methods and implications. Atmos. Environ. 45, 2060–2066.

Chow, J.C., Watson, J.G., Lu, Z., Lowenthal, D.H., Frazier, C.A., Solomon, P.A., et al., 1996. Descriptive analysis of $PM_{2.5}$ and PM_{10} at regionally representative locations during SJVAQS/AUSPEX. Atmos. Environ. 30, 2079–2112.

Chow, J.C., Watson, J.G., Crow, D., Lowenthal, D.H., Merrifield, T., 2001. Comparison of IMPROVE and NIOSH carbon measurements. Aerosol Sci. Technol. 34, 23–34.

Chow, J.C., Watson, J.G., Louie, P.K.K., Chen, L.W.A., Sin, D., 2005. Comparison of $PM_{2.5}$ carbon measurement methods in Hong Kong. China Environ. Pollut. 137, 334–344.

Crounse, J.D., DeCarlo, P.F., Blake, D.R., Emmons, L.K., Campos, T.L., Apel, E.C., et al., 2009. Biomass burning and urban air pollution over the Central Mexican Plateau. Atmos. Chem. Phys. 9, 2699–2734.

Cui, H.F., Mao, P., Zhao, Y., Nielsen, C.P., Zhang, J., 2015. Patterns in atmospheric carbonaceous aerosols in China: emission estimates and observed concentrations. Atmos. Chem. Phys. 15, 8657–8678.

Day, M.C., Zhang, M., Pandis, S.N., 2015. Evaluation of the ability of the EC tracer method to estimate secondary organic carbon. Atmos. Environ. 112, 317–325.

Ding, X., Wang, X.M., Gao, B., Fu, X.X., He, Q.F., Zhao, X.Y., et al., 2012. Tracer-based estimation of secondary organic carbon in the Pearl River Delta, South China. J. Geophys. Res. 117, 2156–2202.

Ding, A.J., Fu, C.B., Yang, X.Q., Sun, J.N., Zheng, L.F., Xie, Y.N., et al., 2013. Ozone and fine particle in the western Yangtze River Delta: an overview of 1 yr data at the SORPES station. Atmos. Chem. Phys. 13, 5813–5830.

Duan, Q., An, J.L., Wang, H.L., Miu, Q., 2014. Pollution characteristics of organic and elemental carbon in atmospheric particles in Nanjing northern suburb in summer. Environ. Sci. 35, 2460–2467 in Chinese.

Feng, Y., Chen, Y., Guo, H., Zhi, G.R., Xiong, S., Li, J., et al., 2009. Characteristics of organic and elemental carbon in $PM_{2.5}$ samples in Shanghai. China Atmos. Res. 92, 434–442.

Folidori, A., Turpin, B.J., Lim, H.J., Cabada, J.C., Subramanian, R., Pandis, S.N., et al., 2006. Local and regional secondary organic aerosol: insights from a year of semi-continuous carbon measurements at Pittsburgh. Aerosol Sci. Technol. 40, 861–872.

Hao, H., Liu, Z., Zhao, F., Li, W., Hang, W., 2015. Scenario analysis of energy consumption and greenhouse gas emissions from China's passenger vehicles. Energy 91, 151–159.

Hu, M., Deng, Z.Q., Wang, Y., Lin, P., Zeng, L.M., Kondo, Y., et al., 2008. Comparison of EC/OC in $PM_{2.5}$ between filter sampling off-line analysis and in situ on-line measurement. Environ. Sci. 29, 3297–3303 in Chinese.

Hu, W.W., Hu, M., Deng, Z.Q., Xiao, R., Kondo, Y., Takegawa, N., et al., 2012. The characteristics and origins of carbonaceous aerosol at a rural site of PRD in summer of 2006. Atmos. Chem. Phys. 12, 1811–1822.

Huebert, B.J., Charlson, R.J., 2000. Uncertainties in data on organic aerosols. Tellus B 52, 1249–1255.

Jung, J.S., Lee, S., Kin, H., Kim, D., Lee, H., Oh, S., 2014. Quantitative determination of the biomass-burning contribution to atmospheric carbonaceous aerosols in Daejeon, Korea, during the rice-harvest period. Atmos. Environ. 89, 642–650.

Latha, K.M., Badarinath, K.V.S., 2004. Correlation between black carbon aerosols, carbon monoxide and tropospheric ozone over a tropical urban site. Atmos. Res. 71, 265–274.

Li, X.H., Wang, S.X., Duan, L., Hao, J.M., Li, C., Chen, Y.S., 2007. Particulate and trace gas emissions from open burning of wheat straw and corn stover in China. Environ. Sci. Technol. 41, 6052–6058.

Li, B., Zhang, J., Zhao, Y., Yuan, S.Y., Zhao, Q.Y., Shen, G.F., et al., 2015. Seasonal variation of urban carbonaceous aerosols in a typical city Nanjing in Yangtze River Delta. China Atmos. Environ. 106, 223–231.

Lim, H.J., Turpin, B.J., 2002. Origins of primary and secondary organic aerosol in Atlanta: results of time-resolved measurements during the Atlanta supersite experiment. Environ. Sci. Technol. 36, 4489–4496.

Lin, P., Hu, M., Deng, Z., Slanina, J., Han, S., Kondo, Y., et al., 2009. Seasonal and diurnal variations of organic carbon in $PM_{2.5}$ in Beijing and the estimation of secondary organic carbon. J. Geophys. Res. 114, 4417–5293.

Ni, H.Y., Han, Y.M., Cao, J.J., Chen, L.W., Tian, J., Wang, X.L., et al., 2015. Emission characteristics of carbonaceous particles and trace gases from open burning of crop residues in China. Atmos. Environ. 123, 399–406.

NJNBS (Nanjing Bureau of Statistics), 2013. Statistical Yearbook of Nanjing. China Statistics Press in Chinese.

NJNBS (Nanjing Bureau of Statistics), 2015. Statistical Yearbook of Nanjing. China Statistics Press in Chinese.

Novakov, T., Menon, S., Kirchstetter, T.W., 2005. Aerosol organic carbon to black carbon ratios: analysis of published data and implications for climate forcing. J. Geophys. Res. 110, 937–946.

Qiu, L.P., 2015. Development and Assessment of the City-scale Emission Inventory of Anthropogenic Air Pollutants: A Case Study of Nanjing MA thesis Nanjing University 2015.

Seinfeld, J.H., Pandis, S.N., 1998. From air pollution to climate change. Atmos. Chem. Phys. 3, 212–214.

Strader, R., Lurmann, F., Pandis, S.N., 1999. Evaluation of secondary organic aerosol formation in winter. Atmos. Environ. 33, 4849–4863.

Tang, L., Yu, H., Ding, A., Zhang, Y., Qin, W., Wang, Z., et al., 2016. Regional contribution to PM_1 pollution during winter haze in Yangtze River Delta. China Sci. Total. Environ. 541, 161–166.

Turpin, B.J., Huntzicker, J.J., 1991. Secondary formation of organic aerosol in the Los Angeles Basin: a descriptive analysis of organic and elemental carbon concentrations. Atmos. Environ. 25, 207–215.

Turpin, B.J., Saxena, P., Andrews, E., 2000. Measuring and simulating particulate organics in the atmosphere: problems and prospects. Atmos. Environ. 34, 2983–3013.

Wang, H.L., Zhu, B., An, J.L., Duan, Q., Zou, J.N., Sheng, L.J., 2014. Size distribution and characterization of OC and EC in atmospheric aerosols during the Asian Youth Games of Nanjing. China Environ. Sci. 35, 3271–3279 in Chinese.

Wang, H.L., Qiao, L.P., Lou, S.R., Zhou, M., Chen, J.M., Wang, Q., et al., 2015a. $PM_{2.5}$ pollution episode and its contributors from 2011 to 2013 in urban Shanghai. China Atmos. Environ. 123, 298–305.

Wang, H.L., Zhu, B., Zhang, Z.F., An, J.L., Shen, L.J., 2015b. Mixing state of individual carbonaceous particles during a severe haze episode in January 2013, Nanjing, China. Particuology 20, 16–23.

Watson, J.G., Chow, J.C., Houck, J.E., 2001. $PM_{2.5}$ chemical source profiles for vehicle exhaust, vegetative burning, geological material, and coal burning in northwestern Colorado during 1995. Chemosphere 43, 1141–1151.

Wilson, R., Spengler, J.D., 1996. Particles in our Air: Concentrations and Health Effects. Harvard University Press, Cambridge, MA.

Wu, M.L., Guo, Z.B., Liu, F.L., Lu, X., Liu, J., Ren, Y.R., 2013. Pollution characteristics and influencing factors of organic and elemental carbon in $PM_{2.1}$ in Nanjing. China Environ. Sci. 33, 1160–1166 in Chinese.

Xiao, R., Takegawa, N., Zheng, M., Kondo, Y., Miyazaki, Y., Miyakawa, T., et al., 2011. Characterization and source apportionment of submicron aerosol with aerosol mass spectrometer during the PRIDE-PRD 2006 campaign. Atmos. Chem. Phys. 11, 6911–6929.

Xu, J.M., Yan, F.X., Xie, Y., Wang, F.Y., Wu, J.B., Fu, Q.Y., 2015. Impact of meteorological conditions on a nine-day particulate matter pollution event observed in December 2013, Shanghai, China. Particuology 20, 69–79.

Yang, H., Yu, J.Z., Ho, S.S.H., Xu, J.H., Wu, W.S., Wan, C.H., et al., 2005a. The chemical composition of inorganic and carbonaceous materials in $PM_{2.5}$, in Nanjing. China Atmos. Environ. 39, 3735–3749.

Yang, F., He, K., Chen, X., Cha, L., Cadle, S.H., Chan, T., et al., 2005b. One-year record of organic and elemental carbon in fine particles in downtown Beijing and Shanghai. Atmos. Chem. Phys. 5, 1449–1457.

Yang, F., Huang, L., Duan, F., Zhang, W., He, K., Ma, Y., et al., 2011a. Carbonaceous species in $PM_{2.5}$ at a pair of rural/urban sites in Beijing, 2005–2008. Atmos. Chem. Phys. 11, 7893–7903.

Yang, F., Tan, J., Zhao, Q., Du, Z., He, K., Ma, Y., et al., 2011b. Characteristics of $PM_{2.5}$ speciation in representative megacities and across China. Atmos. Chem. Phys. 11, 5207–5219.

Yao, X., Chan, C.K., Fang, M., Cadle, S., Chan, T., Mulawa, P., et al., 2002. The water-soluble ionic composition of $PM_{2.5}$ in Shanghai and Beijing. China Atmos. Environ. 36, 4223–4234.

Yao, Z., Wu, B., Wu, Y., Cao, X., Jiang, X., 2015. Comparison of NOx emissions from China III and China IV in-use diesel trucks based on on-road measurements. Atmos. Environ. 15, 1352–2310.

Yuan, Z.B., Yu, J.Z., Lau, A.K.H., Louie, P.K.K., Fung, J.C.H., 2006. Application of positive matrix factorization in estimating aerosol secondary organic carbon in Hong Kong and its relationship with secondary sulfate. Atmos. Chem. Phys. 6, 25–34.

Yuan, S.Y., Shen, G.F., Zhao, Q.Y., 2014. Concentrations and distribution characteristics of organic carbon and element carbon in ambient particulate matter (PM_{10} and $PM_{2.5}$) during autumn in Nanjing. Environ. Chem. 33, 724–730 in Chinese.

Zhang, F.W., Zhao, J.P., Chen, J.S., Xu, Y., Xu, L.L., 2011. Pollution characteristics of organic and elemental carbon in $PM_{2.5}$ in Xiamen. China J. Environ. Sci. 23, 1342–1349.

Zhang, Y.Y., Yu, M.X., Ren, L., Zhu, Z.F., 2012. Organic and element carbon pollution characteristics of atmospheric fine particles in Nanjing. Admin. Tech. Environ. Monitor. 24, 30–32 in Chinese.

Zhang, Y.J., Tang, L.L., Yu, H.X., Wang, Z., Sun, Y.L., Qin, W., et al., 2015. Chemical composition, sources and evolution processes of aerosol at an urban site in Yangtze River Delta, China during wintertime. Atmos. Environ. 123, 339–349.

Zhang, Y., Huang, W., Cai, T., Fang, D., Wang, Y., Song, J., et al., 2016. Concentrations and chemical compositions of fine particles ($PM_{2.5}$) during haze and non-haze days in Beijing. Atmos. Res. 174, 62–69.

Zhao, M.F., Qiao, T., Huang, Z.S., Zhu, M.Y., Xu, W., Xiu, G.G., et al., 2015a. Comparison of ionic and carbonaceous compositions of $PM_{2.5}$ in 2009 and 2012 in Shanghai. China Sci. Total. Environ. 536, 695–703.

Zhao, Y., Qiu, L.P., Xu, R.Y., Xie, F.J., Zhang, Q., Yu, Y.Y., 2015b. Advantages of a city-scale emission inventory for urban air quality research and policy: the case of Nanjing, a typical industrial city in the Yangtze River Delta. China Atmos. Chem. Phys. 15, 12623–12644.

Zhuang, B.L., Wang, T.J., Liu, J., Li, S., Xie, M., Yang, X.Q., et al., 2014. Continuous measurement of black carbon aerosol in urban Nanjing of Yangtze River Delta. China Atmos. Environ. 89, 415–424.

Zielinska, B., Sagebiel, J., McDonald, J.D., Whitney, K., Lawson, D.R., 2012. Emission rates and comparative chemical composition from selected in-use diesel and gasoline-fueled vehicles. J. Air Waste Manage. Assoc. 54, 1138–1150.